EVALUATION OF ANISOTROPIC DEFORMATION AND FRACTURE PROPERTIES IN EXTRUDED HAP/PLLA COMPOSITES

Mototsugu Tanaka[1], Hidekazu Tanaka[2], Masaki Hojo[2], Taiji Adachi[2]
Suong-Hyu Hyon[3] and Masakazu Konda[4]

[1] Department of Aeronautics, Kanazawa Institute of Technology
7-1, Ohgigaoka, Nonoichi, Ishikawa 921-8501, Japan
mototsugu@neptune.kanazawa-it.ac.jp
[2] Department of Mechanical Engineering & Science, Kyoto University
[3] Institute for Frontier Medical Sciences, Kyoto University
[4] BMG Inc.

ABSTRACT

The biocompatible composite materials composed of hydroxyapatite (HAp) and poly-L-lactic acid (PLLA) are strong candidates of scaffold materials for a novel bone regeneration technology. In the present paper, the static tensile tests and fracture toughness tests were carried out for uniaxially-extruded neat PLLA and HAp/PLLA composites, in order to evaluate the basic deformation and fracture properties. The oriented molecular- and micro- structures, which were introduced by the hydrostatic pressure extrusion molding, brought the anisotropy in elastic modulus, tensile strength and fracture toughness. The elastic modulus increased by adding HAp to PLLA. Specially, the elastic modulus of the HAp short fiber/PLLA composite was more than 10 GPa. The tensile strength and fracture toughness of HAp/PLLA composites were lower than those of neat PLLA owing to low interfacial strength. In addition, the anisotropy in the deformation and fracture properties was discussed from the microstructural viewpoint. It is suggested that the HAp short fiber is more effective as reinforcement material than HAp particle owing to the higher stress transfer ability originated by its high aspect ratio.

1. INTRODUCTION

A novel bone regeneration technology is expected to be developed using scaffolds and activities of bone-forming cells, instead of the traditional bone filling surgery [1]. Here, the cellular bone formation activities are accelerated by the transplantation of porous scaffold materials as bone filling substitutes, resulting in the complete bone regeneration by hydrolytic resorption of scaffold materials and replacement to newly formed bone [2]. The biocompatible composite materials composed of hydroxyapatite (HAp) and poly-L-lactic acid (PLLA) are strong candidates for scaffold materials, owing to their bone-conductivity and biodegradability [3, 4].

The poor fracture properties [5] are one of the factors limiting their practical application. In order to improve their fracture properties, the uniaxially-extruded HAp/PLLA composites had been recently developed via the hydrostatic pressure extrusion molding [6]. It is necessary to understand the relation between the deformation/fracture properties and the microstructure anisotropy to establish the microstructural designing principle.

In the present study, the static tensile tests and fracture toughness tests were carried out for uniaxially-extruded neat PLLA and HAp/PLLA composites to evaluate the basic deformation and fracture properties. The anisotropy in the deformation and fracture properties was discussed from the microstructural viewpoint.

2. MATERIALS AND METHODS

The HAp particles (Ube Material Industries) and HAp short fibers (Ube Material Industries) were used as the fillers, and PLLA (BMG Inc.) was used as matrix. The

initial molecular weight of PLLA was about 2.4×10^5. The rods (length: 430 mm, diameter: 7.5 mm, extrusion ratio: 4) of neat PLLA and HAp/PLLA composites (HAp: 14 vol%) were prepared using the hydrostatic pressure extrusion molding [6].

After material preparation, the molecular weight was measured using a gel permeation chromatography (Shimadzu, LC-6A/CTO-10A/RID6A/C-R4A). The crystallinity was measured using a differential scanning calorimetry (Shimadzu, DSC-50). The anisotropy in crystal structure was evaluated using an X-ray diffractometer (Rigaku, RINT2000). The anisotropy in mesoscopic structure was observed using a scanning electron microscope (SEM: JEOL, JSM-5400LS) and a field-emission scanning electron microscope (FE-SEM: Hitachi, S-4500).

Static tensile tests and fracture toughness tests were carried out using a universal testing machine (Shimadzu, Autograph AG 50-kNG) with a load cell of 1 kN in capacity. The crosshead speed was 1 mm/min. Deformation was measured using a video extensometer (Shimadzu, DVE-200) both for static tensile tests and fracture toughness tests. Specimens both parallel (0°-specimen) and perpendicular (90°-specimen) to the extrusion direction were prepared. The size of 0°- and 90°- specimens for static tensile tests was 2 (width) × 0.5 (thickness) × 12 (gauge length) mm and 2 (width) × 0.5 (thickness) × 3 (gauge length) mm, respectively. For fracture toughness tests, double edge notched tension (DENT) specimens were prepared. The size of 0°- and 90°-specimens for fracture toughness tests was 2 (width) × 0.5 (thickness) × 25 (gauge length) mm and 2 (width) × 0.5 (thickness) × 7 (gauge length) mm, respectively. The notches with radius of about 7 μm were introduced using precision needle files. The nominal depth was 0.5 mm and 0.2 mm for 0°- and 90°- specimens, respectively. In this study, J-integral was calculated using maximum load for the evaluation of fracture toughness. J-integral for DENT specimen is expressed as follows.

$$J_{\mathrm{I}} = \frac{K_{\mathrm{I}}^{\,2}}{E} + \frac{2}{bB}\left[\int_0^{\delta} P d\delta - \frac{P\delta}{2}\right] \qquad (1)$$

Here, E is elastic modulus, b is length of ligament portion, B is specimen thickness, P is load, δ is deformation of loading point, and K_{I} is stress intensity factor. Fracture surfaces after fracture toughness tests were observed using a SEM and a FE-SEM.

3. RESULTS AND DISCUSSION

3.1 Molecular- and Micro- Structures

Measured molecular weight and crystallinity are shown in Table 1. Molecular weight was decreased by chain scission during material preparation. Figure 1 shows an X-ray diffraction image of a neat PLLA rod. X-ray diffraction image indicated the molecular structure in the hydrostatic-pressure-extrusion-molded rods was highly oriented to the extrusion direction.

Table 1: Molecular weight and crystallinity of neat PLLA and HAp/PLLA composites.

Material	Molecular weight	Crystallinity
Neat PLLA	1.7×10^5	48%
HAp particle/PLLA	8.6×10^4	53%
HAp short fiber/PLLA	1.3×10^5	57%

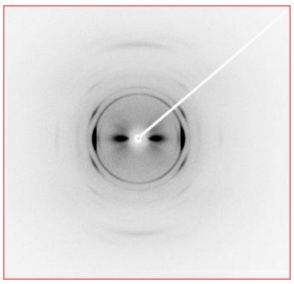

Figure 1: X-ray diffraction image of a neat PLLA rod.

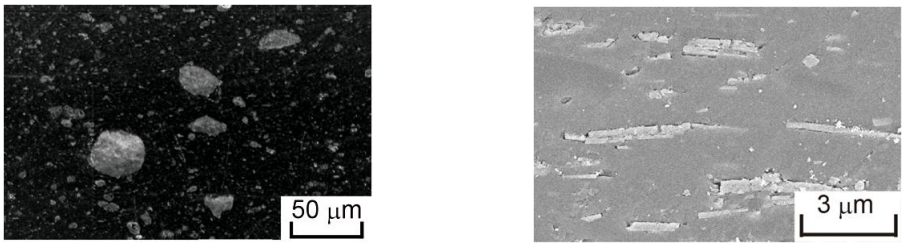

a) b)

Figure 2: Cross sectional areas of a) HAp particle/PLLA composite and b) HAp short fiber/PLLA composite.

Figure 2 indicates the microstructure of HAp/PLLA composites. HAp particle size had large scatter. The average and maximum size of HAp particles were about 5 μm and more than 30 μm, respectively. On the other hand, the HAp short fibers had higher aspect ratio and smaller size than those of the HAp particles, and were almost uniaxially oriented in the extrusion direction. Many interfacial defects were observed between HAp short fibers and PLLA matrix.

3.2 Effect of Microstructural Anisotropy on Elastic Modulus

Figure 3 (a) shows representative stress-strain curves of 0°- specimens for static tensile tests. Neat PLLA shows large plastic deformation. On the other hand, the fracture strain decreased by adding HAp to PLLA. Figure 3 (b) shows representative stress-strain curves of 90°- specimens for static tensile tests. The 90°- specimens fractured without yield behaviour.

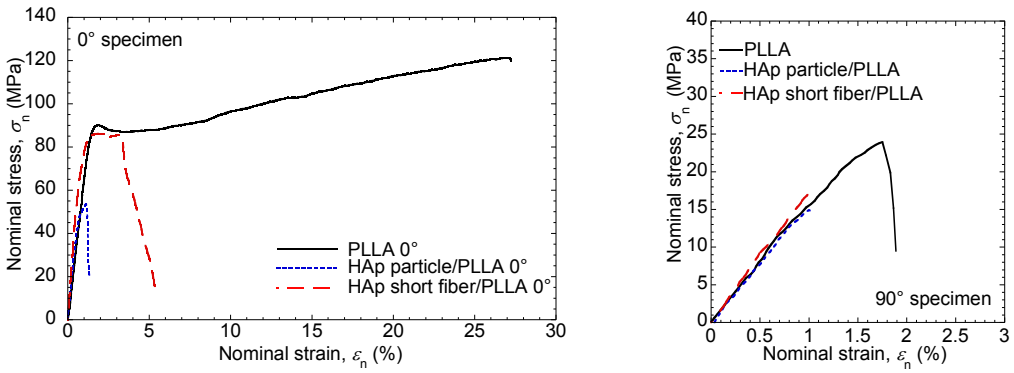

a) b)

Figure 3: Tensile stress-strain curves of a) 0°- specimens and b) 90°- specimens.

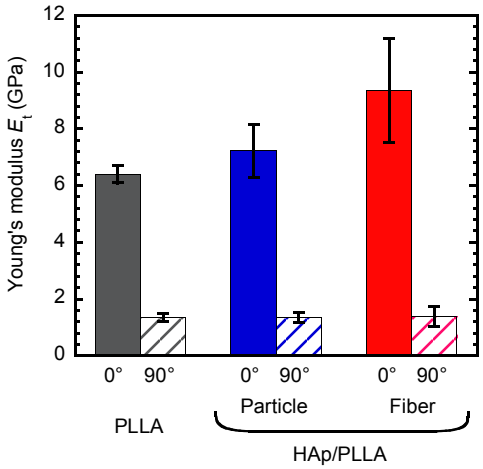

Figure 4: Elastic modulus of neat PLLA and HAp/PLLA composites.

Figure 4 indicates the elastic modulus obtained by static tensile tests. The elastic modulus of 0°- specimen for neat PLLA (6.4 GPa) is much higher than that reported in the former work (2 GPa) [7]. On the other hand, the elastic modulus of 90°- specimen for neat PLLA was 1.4 GPa. Thus, the oriented molecular structure, which was introduced by the hydrostatic pressure extrusion molding, brought the anisotropy in elastic modulus of neat PLLA.

The elastic modulus increased by adding HAp, for 0°-specimen. Specially, the elastic modulus of the HAp short fiber/PLLA composite was more than 10 GPa, but was still less than that expected by the rule of mixture. Thus, it is suggested that the increase in the aspect ratio of HAp fibers and the decrease in interfacial defects could improve the stiffness of HAp/PLLA composites. On the other hand, the elastic modulus for HAp/PLLA composites (10-20 % of 0°-specimen) was almost the same as that for neat PLLA for 90°-specimen. It is suggested the elastic modulus of 90°-specimen was governed by the molecular chains direction of PLLA matrix.

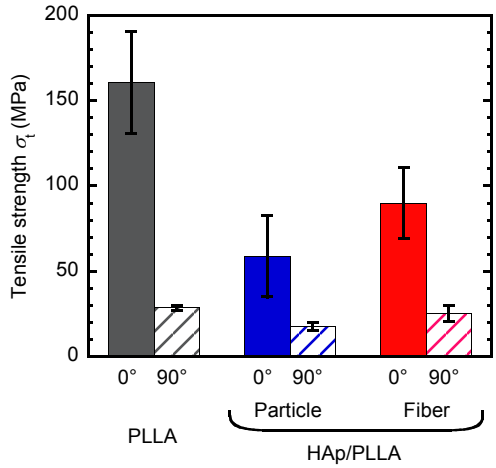

Figure 5: Tensile strength of neat PLLA and HAp/PLLA composites.

3.3 Effect of Microstructural Anisotropy on Tensile Strength

Figure 5 indicates the tensile strength obtained by static tensile tests. For 0°-specimen, the tensile strength of HAp particle/PLLA and HAp short fiber/PLLA composites was

about 40 % and 60 % of that of neat PLLA, respectively. On the other hand, the tensile strength of HAp/PLLA composites (around 25 % of 0°-specimen) was almost same as that of neat PLLA, for 90°-specimen. The strength of 90°-specimen was also governed by PLLA matrix. Thus, the anisotropy was large in the tensile strength.

3.4 Effect of Microstructural Anisotropy on Fracture Toughness

Since the 0°-specimen of neat PLLA did not satisfy the small scale yielding condition, J-integral was used for the evaluation of fracture toughness. Figure 6 indicates the obtained fracture toughness. For the 0°-specimen, the fracture toughness of HAp particle/PLLA and HAp short fiber/PLLA composites was 35 % and 85 % of that of neat PLLA, respectively. It is suggested the HAp fiber is more effective as reinforcement material than HAp particle owing to the higher stress transfer ability due to its high aspect ratio. For the 90°-specimen, the fracture toughness was extremely low (less than 5 % of 0°-specimen). The fracture toughness of HAp/PLLA composites was almost the same as that of neat PLLA, for 90°-specimen. Thus, the fracture toughness of 90°-specimen was also governed by PLLA matrix, and the anisotropy was large in the fracture toughness.

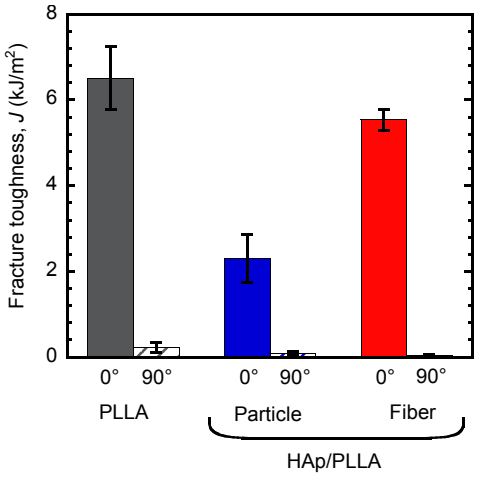

Figure 6: Fracture toughness of neat PLLA and HAp/PLLA composites.

Thus, the effect of microstructural anisotropy on fracture toughness was different from that on tensile strength. First, the ratio of '90°-specimen' to '0°-specimen' in fracture toughness (about 0.03) was smaller than that in tensile strength (about 0.18), for neat PLLA. In Equation (1), the first term is in proportion to the stress intensity factor. This means the first term in Equation (1) is in proportion to the square of the maximum load. Therefore, the effect of microstructural anisotropy on fracture toughness of neat PLLA was larger than that on tensile strength. Actually, the square of the ratio of '90°-specimen' to '0°-specimen' in tensile strength roughly agrees to the ratio of '90°-specimen' to '0°-specimen' in fracture toughness for neat PLLA.

On the other hand, the ratio of '90°-specimen' to '0°-specimen' in fracture toughness (much less than 0.05) was much smaller than the square of the ratio of '90°-specimen' to '0°-specimen' in tensile strength (about 0.06), for HAp/PLLA composites. This tendency is much evident for HAp short fiber/PLLA composite. Furthermore, the decreasing rate in fracture toughness by adding HAp short fibers to PLLA was smaller than that in tensile strength, for 0°-specimen. The reason for this deference, originated by the shape of HAp, will be discussed in next section.

3.5 Effect of Microstructural Anisotropy on Fracture Process

Figures 7 and 8 show fracture surfaces after fracture toughness tests. Figures 9 and 10 indicate the schematic of fracture process suggested from the fracture surface observation. First, fracture surfaces of 0°-specimen is discussed. For neat PLLA, the evidence of plastic deformation was observed along the extrusion direction. This means that cracks propagated at intermediate portion between oriented PLLA microstructures (for example, tie chains between crystal phases) in the case of neat PLLA. On the other hand, HAp particles and fibers were observed on the fracture surfaces for HAp/PLLA composites with interfacial debonding. This means that cracks propagated also at interface between HAp and PLLA. This was due to the low interfacial strength caused by initial interfacial defects, resulting in low fracture properties for HAp/PLLA composites. Thus, the interfacial control hopefully improves the tensile strength of HAp/PLLA composites. While the evidence of plastic deformation was scarcely observed for HAp particle/PLLA composite, the evidence of plastic deformation was observed along the extrusion direction for HAp short fiber/PLLA composite. HAp fibers prevented the crack propagation owing to their higher aspect ratio, resulting in relatively higher tensile strength and fracture toughness of HAp short fiber/PLLA composite than that of HAp particle/PLLA composite. Furthermore, the plastic deformation of PLLA matrix contributed to the smaller decreasing rate in fracture toughness by adding HAp short fibers to PLLA than that in tensile strength.

Secondary, fracture surfaces of 90°-specimens are compared with those of 0°-specimens. For neat PLLA, the evidence of plastic deformation was observed along the extrusion direction similarly to 0°-specimen. On the other hand, the evidence of plastic deformation was scarcely observed for HAp/PLLA composites. In addition, HAp particles and fibers were scarcely observed for HAp/PLLA composites. This means that crack propagated at extremely weak intermediate portion between oriented PLLA microstructure for 90°-specimen of neat PLLA and HAp/PLLA composites. Therefore, the ratio of '90°-specimen' to '0°-specimen' in fracture toughness (much less than 0.05) was much smaller than the square of the ratio of '90°-specimen' to '0°-specimen' in tensile strength (about 0.06), for HAp/PLLA composites.

4. CONCLUSIONS

In this study, the static tensile tests and fracture toughness tests were carried out for uniaxially-extruded neat PLLA and HAp/PLLA composites in order to evaluate the basic deformation and fracture properties. In addition, the anisotropy in the deformation and fracture properties was discussed from the microstructural viewpoint. The results are summarized as follows.

(i) The oriented molecular- and micro- structures, which were introduced by the hydrostatic pressure extrusion molding, brought the anisotropy on elastic modulus of neat PLLA.

(ii) The elastic modulus increased by adding HAp, for 0°-specimen. Specially, the elastic modulus of the HAp short fiber/PLLA composite was more than 10 GPa.

(iii) The tensile strength and fracture toughness of HAp/PLLA composites were lower than those of neat PLLA owing to low interfacial strength.

(iv) It is suggested the HAp fiber is more effective than HAp particle as reinforcement material owing to the higher stress transfer ability originated by its high aspect ratio.

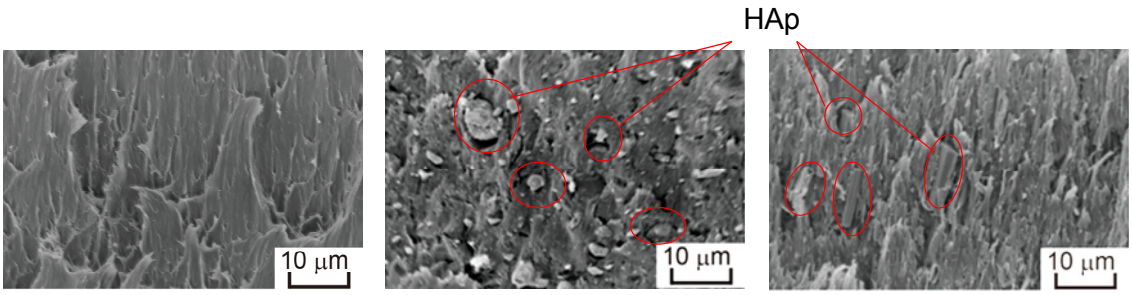

a) b) c)

Figure 7: Fracture surfaces of 0°- specimens for a) neat PLLA, b) HAp particle/PLLA and c) HAp short fiber/PLLA.

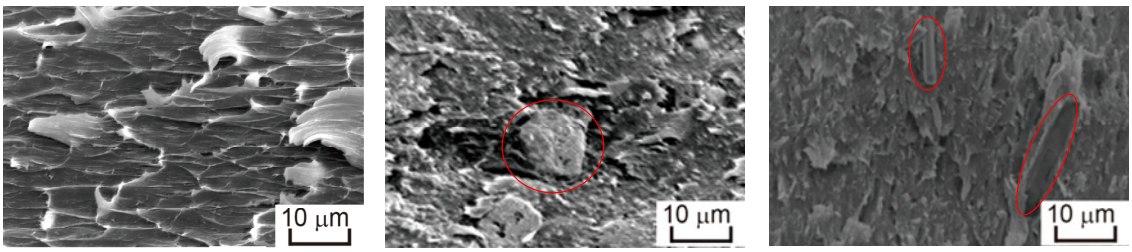

a) b) c)

Figure 8: Fracture surfaces of 90°- specimens for a) neat PLLA, b) HAp particle/PLLA and c) HAp short fiber/PLLA.

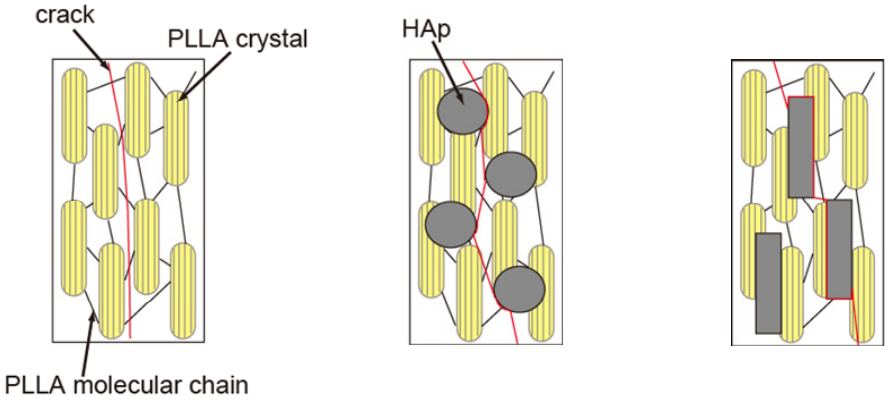

a) b) c)

Figure 9: Schematics of fracture process of 0°- specimens for a) neat PLLA, b) HAp particle/PLLA and c) HAp short fiber/PLLA.

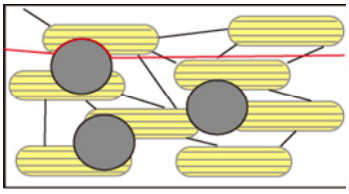

Figure 10: Schematics of fracture process of 90°- specimens.

ACKNOWLEDGEMENTS
The authors gratefully acknowledge Prof. Takashi Nishino (Kobe University) for his help with the X-ray diffraction measurement. The authors also acknowledge Mr. Osamu Nishimura (Imoto, Co. Ltd.) for his helpful discussion. Furthermore, the authors acknowledge Mr. Sadamu Kinoshita (Kyoto University) for his help with FE-SEM observation.

REFERENCES

1- Hutmacher, D.W., Schantz, T., Zein, I., Ng, K.W., Teoh, S.H., Tan, K.C., *Journal of Biomedical Materials Research*, 2001;55: 203-216.
2- Adachi T., Osako, Y., Tanaka, M., Hojo, M., Hollister, S.J., *Biomaterials*, 2006;27: 3964-3972.
3- Ignjatović N., Tomić, S., Dakić, M., Miljković, M., Plasvić, M., Uskoković, D., *Biomaterials*, 1999;20:809-816.
4- Shikinami, Y., Okuno, M., *Biomaterials*, 1999;20:859-877.
5- Todo M., Park, S.D., Arakawa, K., Takenoshita, Y., *Composites: Part A*, 2006;37:2221-2225.
6- Jin F., Moon, S.I., Tsutsumi, S., Hyon, S.H., *Macromolecular Symposia*, 2005;224:93-104.
7- Hyon, S.H., Jin, F., Jamshidi, K., Tutumi, S., Kanamoto, T., *Macromolecular Symposia*, 2003;197:355-368.